Metabolic Engineering 42 (2017) 25–32

Contents lists available at ScienceDirect

Metabolic Engineering

journal homepage: www.elsevier.com/locate/meteng

Biosynthesis of plant-derived ginsenoside Rh2 in yeast via repurposing a key promiscuous microbial enzyme

Yu Zhuang[a,1], Guang-Yu Yang[a,1], Xiaohui Chen[a], Qian Liu[a], Xueli Zhang[b], Zixin Deng[a], Yan Feng[a,*]

[a] State Key Laboratory of Microbial Metabolism, School of Life Sciences and Biotechnology, Shanghai Jiao Tong University, Shanghai 200240, China
[b] Tianjin Institute of Industrial Biotechnology, Chinese Academy of Sciences, Tianjin 300308, China

ARTICLE INFO

Keywords:
Ginsenoside
Glycosyltransferase
Enzyme promiscuity
Protein engineering
Metabolic engineering
Synthetic biology

ABSTRACT

Ginsenoside Rh2 is a potential anticancer drug isolated from medicinal plant ginseng. Fermentative production of ginsenoside Rh2 in yeast has recently been investigated as an alternative strategy compared to extraction from plants. However, the titer was quite low due to low catalytic capability of the key ginseng glycosyltransferase in microorganisms. Herein, we have demonstrated high-level production of ginsenoside Rh2 in *Saccharomyces cerevisiae* via repurposing an inherently promiscuous glycosyltransferase, UGT51. The semi-rationally designed UGT51 presented an ~1800-fold enhanced catalytic efficiency (k_{cat}/K_m) for converting protopanaxadiol to ginsenoside Rh2 *in vitro*. Introducing the mutant glycosyltransferase gene into yeast increased Rh2 production from 0.0032 to 0.39 mg/g dry cell weight (DCW). Further metabolic engineering, including preventing Rh2 degradation and increasing UDP-glucose precursor supply, increased Rh2 production to 2.90 mg/g DCW, which was more than 900-fold higher than the starting strain. Finally, fed-batch fermentation in a 5-L bioreactor led to production of ~300 mg/L Rh2, which was the highest titer reported.

1. Introduction

Ginseng saponins have well-known therapeutic functions, and ginseng plants have been widely cultivated in North America and Asia. Ginsenoside Rh2 is a trace but important saponin isolated from red ginseng (Kitagawa et al., 1983), and it exhibits diverse pharmacological effects, such as anti-oxidation, hepatoprotection, anti-diabetes and anti-tumor (Hwang et al., 2007; Kim et al., 1999; Liu, 2012). The use of Rh2 in combination with anti-tumor drugs remarkably increased the efficacy of tumor suppression and reduced the side effects caused by chemotherapy (Nakata et al., 1998). Despite the versatile bioactivities of ginsenoside Rh2, its content in red ginseng is extremely low (around 0.001%) (Shibata, 2001). Currently, ginsenoside Rh2 is primarily manufactured by chemical or biological deglycosylation of ginsenosides (Bae et al., 2004; Su et al., 2006; Zhang et al., 2001). Because of the long cultivation periods for qualified roots (5–7 years) and the complicated extraction and purification process, the preparation of ginsenoside Rh2 requires considerable time and labor costs.

With the development of synthetic biology, substantial progress has been made in the low-cost production of plant natural products in microbes, including artemisinin (Martin et al., 2003), Taxol (Ajikumar et al., 2010), strictosidine (Brown et al., 2015), and opioids (Galanie et al., 2015). These plant-derived compounds are synthesized in microbial host cells via the establishment of non-inherent synthetic pathways. Recently, microbial production of protopanaxadiol (PPD), the precursor of ginsenoside Rh2, in *S. cerevisiae* was reported (Dai et al., 2013). Subsequently, heterologous production of ginsenoside Rh2 was accomplished by introducing ginseng glycosyltransferase UGTPg45 in *S. cerevisiae*. However, the titer was quite low (~16 mg/L) because of the unsatisfied performance of the key ginseng glycosyltransferase as kinetic parameters measured (Wang et al., 2015). Comparable accumulation of PPD precursor within the engineered yeast strains suggested that the glycosyltransferase involved in the last step was the bottleneck in the whole pathway. Therefore, it was essential to increase glycosyltransferase activity towards Rh2 synthesis.

Besides using plant-derived glycosyltransferase, an alternative way is to use engineered substrate-promiscuous enzymes (Dietrich et al., 2009). Microbial enzymes commonly exhibit 'substrate promiscuity', which represents an evolutionary locus for adapting to varied environments and enables microbes to perform comparable chemical transformations using different substrates (Copley, 2015). Promiscuous microbial enzymes can interact with a variety of substrates that have

* Corresponding author.
E-mail address: yfeng2009@sjtu.edu.cn (Y. Feng).
[1] These authors contributed equally to this work.

http://dx.doi.org/10.1016/j.ymben.2017.04.009
Received 28 February 2017; Received in revised form 13 April 2017; Accepted 26 April 2017
Available online 04 May 2017

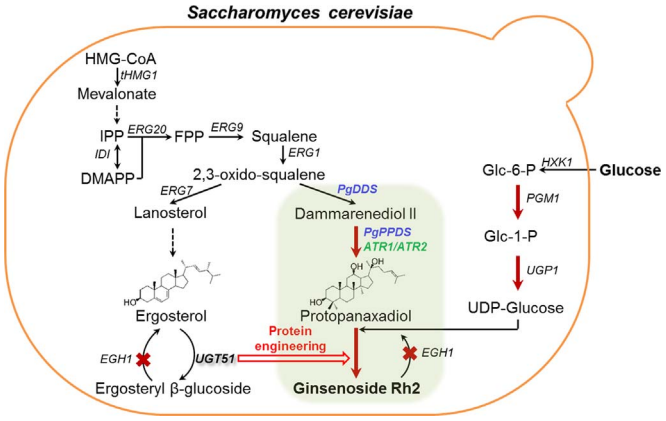

Fig. 1. Designed biosynthetic pathway of ginsenoside Rh2 in yeast. Steryl-glucoside and ginsenoside Rh2 were both derived from 2,3-oxidosqualene via similar reactions, including cyclization, hydroxylation and glycosylation. Yeast genes are shown in black. Genes from *P. ginseng* are shown in blue. Genes from *A. thaliana* are shown in green. Multiple-step reactions are shown as dashed arrows, and overexpressed steps are shown as bold arrows. Abbreviations: HMG-CoA, 3-hydroxy-3-methylglutaryl coenzyme A; IPP, isopentenylpyrophosphate; DMAPP, dimethylallylpyrophosphate; FPP, farnesyldiphosphate; Glu-6-P, Glucose 6-phosphate; and Glu-1-P, Glucose 1-phosphate.

structures similar to their natural substrates, although the activity may be lower with the non-natural substrates. Nonetheless, these enzymes native to the chassis cells represent good candidates for further directed evolution, which may lead to the desired performance both *in vitro* and *in vivo*.

To identify the promiscuous microbial enzyme candidates for Rh2 synthesis, we performed a comparative analysis of saponins between steryl-glucoside biosynthetic pathway in *S. cerevisiae* and ginsenoside Rh2 biosynthetic pathway from ginseng (Fig. 1). UGT51 is a UDP-glucose: sterol glucosyltransferase from *S. cerevisiae*, and it is responsible for the glucosylation of ergosterol to form ergosteryl-glucoside. Moreover, UGT51 has been reported to enable the conversion of certain sterols into steryl-glucosides (Warnecke et al., 1999). Accordingly, we presumed that the promiscuous UGT51 native to the chassis cell may serve as a promising starting enzyme for microbial production of plant saponins. In the present study, high production of ginsenoside Rh2 represented an excellent example of *de novo* biosynthesis of plant natural products in microbes via the use of an engineered promiscuous microbial enzyme.

2. Materials and methods

2.1. Chemicals, strains and culture conditions

PPD, dammarenediol II and other acceptor compounds (> 98% purity) were obtained from Faces Biochemical (Wuhan, China). Ginsenoside Rh2 was purchased from Sigma-Aldrich (USA), and 2-chloro-4-nitrophenyl β-D-glucopyranoside was synthesized by WuXi AppTec (China).

E. coli BL21 CodonPlus (*DE3*) cells were used as the host cells for the expression of the UGTs. The yeast chassis strain ZD-PPD-016(URA3$^-$) (Dai et al., 2013) was kindly provided by Prof. Zhang at Tianjin Institute of Industrial Biotechnology. The plasmid pUMRI-10 (Xie et al., 2015) was kindly provided by Prof. Yu at Zhejiang University. All plasmids and strains used in this study are listed in Table S1 and S2, and they were constructed as described in the Supplementary Data. All of the primers used for plasmid and strain construction are listed in Table S3.

Shake-flask cultures for the yeast strains are described in the Supplementary Data. The fed-batch fermentations were performed in a 5-L bioreactor (WinPact, USA) with an initial working volume of 2 L. The media for seed and batch fermentation were modified from previously described media (Lenihan et al., 2008), and 5g/L of lysine was added. The seed culture was inoculated with a fermenter with an initial OD_{600} of 0.5. The initial agitation was set to 300 rpm and increased to a maximum of 800 rpm. Fermentation was conducted as previously described (Dai et al., 2013). The glucose and ethanol concentrations were measured with an SBA-40E Biosensor (Institute of Biology, Academy of Sciences, Shandong, China) according to the manufacturer's instructions.

2.2. Production and purification of glucosyltransferase UGT51

The gene fragment of UGT51 excluding the first 721 N-terminal amino acids (Warnecke et al., 1999) was amplified from the chromosome of *S. cerevisiae* S288c as the template using the primer sets UGT51_F (5'-CAAGCATATGTTAATGATTGATGAGAATCCGC-3') and UGT51_R (5'-CTAGCTCGAGTTAAATCATCGTCCACCCTTCA-3'), which incorporated *NdeI* and *XhoI* sites, respectively. The amplified gene was ligated into the pET-28a vector (Novagen). The recombinant plasmid was then transformed into *E. coli* BL21 CodonPlus cells for expression.

The cells were grown at 37 °C in 1 L of LB medium containing 50 μg/mL of kanamycin and 34 μg/mL of chloramphenicol to an OD_{600} of 0.6–0.8. Induction was performed by adding 0.4 mM isopropyl-1-thio-*b*-D-galactopyranoside (IPTG), and further incubation was performed for 20 h at 16 °C. The cells were harvested by centrifugation (5000 × *g*, 4 °C) and resuspended in 100 mL of lysis buffer (20 mM Tris-HCl, pH 8.0, 2 mM 1,4-dithiothreitol). Cell disruption was performed by ultrasonication. The cell extracts were applied to a 2-mL Ni Sepharose™ 6 Fast Flow column (GE Healthcare), which was pre-equilibrated in buffer A (20 mM Tris-HCl, pH 8.0, 500 mM NaCl). After extensive washing, fractions were eluted using 5 column volumes of buffer A containing 120 mM imidazole.

2.3. Glycosyltransferase assay

The reaction mixture for the PPD enzymatic assay consisted of 100 μl of 20 mM Tris-HCl buffer (pH 8.0) containing PPD (0.5 mM), UDP-glucose (5 mM), 1% (v/v) Tween80 and 0.2 mg/mL purified glycosyltransferase. For the kinetic study, the concentration of PPD ranged from 0.05 to 1 mM. The mixture was incubated in a thermal shaker at 37 °C and 200 rpm. The reaction was terminated by the addition of the same volume of *n*-butanol. The product was extracted and evaporated, and the residue was dissolved in methanol for the HPLC analysis. The lipids were injected on an Agilent1260 HPLC with UV detection at 203 nm using an Agilent Eclipse XDB-C18 (5 μm, 4.6 × 250 mm) column. The solvent flow rate was 1.0 mL/min and the column temperature was set at 40 °C. The mobile phase consisted of water (A) and acetonitrile (B), and a gradient program of 45–100% B in 0–14 min, 100% B in 14–18 min, and 45% B in 18–20 min was applied.

The reaction mixture for the acceptor specificity determination consisted of 100 μl of 20 mM Tris-HCl buffer (pH 8.0) containing the acceptor (0.5 mM), UDP-glucose (2 mM), 1% (v/v) Tween80 and 0.3 mg/mL purified glycosyltransferase. The mixture was incubated in a thermal shaker at 37 °C and 200 rpm and terminated by the addition of *n*-butanol in 2 h. An HPLC analysis was performed to quantify the conversion of the acceptor in each reaction. The conditions for the HPLC analysis were the same as those mentioned above and excluded the mobile phase. In the case of ergosterol, cholesterol, sitosterol and diosgenin, the mobile phase consisted of acetonitrile, methanol and propanol at the volume ratio of 50:80:10. The mobile phase for protopanaxatriol and mogrol was the same as that of PPD. The mobile phase for estradiol and pregnenolone consisted of water (A) and acetonitrile (B), and a gradient program of 10% B in 0–3 min, 10–100% B in 3–20 min, 100% B in 20–23 min, and 10% B in 23–25 min was applied.

2.4. Chemical analysis

The reaction products with PPD as the substrate were dissolved in chloroform/methanol (85/15, v/v) for purification by Silica Gel 60 (Merck KGaA, Darmstadt, Germany) using chloroform/methanol (85/15, v/v) as the elution solvent. The structural identification of the purified products was conducted by ^{1}H NMR and ^{13}C NMR (Bruker AV-400 spectrometer). All NMR spectra were obtained in pyridine-d_5.

2.5. Site-directed mutagenesis and iterative saturation mutagenesis

Alanine scanning mutagenesis, a method of systematic alanine substitution, was particularly useful for the identification of functional residues. All the selected residues are individually mutated to alanine using the GCG codon for removing all side-chain atoms past the β-carbon. The primers used for alanine scanning are shown in Table S4. All mutants were created in the recombinant vector pET28a-UGT51. The PCR assay was conducted with PrimeSTAR DNA polymerase (TaKaRa). The product was subsequently treated with *DpnI* for 2 h at 37 °C and transformed into *E. coli* BL21 CodonPlus (*DE3*) cells. The targeted mutation was confirmed by sequencing. Soluble fractions of the enzymes were obtained after cell sonication and then purified by the method mentioned above. The relative activities were measured using the wild type as the control.

The pET28a-UGT51 plasmid was used as the initial template for iterative saturation mutagenesis using the NNK codon. All primers are shown in Table S4. To screen all the single amino acid exchange mutants, a sufficient number of colonies (200 colonies at one site) were examined. The high-throughput assay for glycosyl transfer was performed based on a previously described method (Gantt et al., 2011). The reaction mixture consisted of 100 μl of 20 mM Tris-HCl buffer (pH 8.0) containing PPD (0.25 mM), 2-chloro-4-nitrophenyl β-D-glucopyranoside (0.5 mM), UDP-Glucose (1 mM), 1% (v/v) Tween80, 11 μM OleD variant TDP-16 (containing mutations P67T S132F A242L Q268V), and 50 μl UGT enzyme solution. The microplates were incubated at 30 °C, and the reaction progress was monitored at 410 nm over 20 min.

2.6. Metabolite analysis

The cell pellets were harvested, disrupted and extracted with *n*-butanol and used for the analysis of intracellular dammarenediol II, PPD and Rh2 by HPLC at the same conditions as in "2.3 Glycosyltransferase assay". The supernatant was extracted directly with *n*-butanol and used for the analysis of extracellular dammarenediol II, PPD and Rh2 by HPLC. The titers refer to the sum of the intracellular and extracellular contents. The structures of metabolites produced by the engineered yeast strains were further confirmed by HPLC/ESIMS. High-resolution ESIMS data was acquired using an Agilent 1290-MS 6230 TOF-MS system with positive model.

3. Results

3.1. UGT51 from S. cerevisiae is a promiscuous glucosyltransferase for Rh2 synthesis

To identify whether the inherent glycosyltransferase UGT51 could catalyze conversion of the unnatural substrate PPD, the gene encoding the catalytic domain of UGT51, was overexpressed in *Escherichia coli* BL21 CodonPlus (*DE3*) cells and purified (Fig. S1). Then the *in vitro* assays were carried out with various acceptors as listed in Fig. 2A, and each conversion ratios were calculated according to the amounts of remaining acceptors that were quantified by HPLC analysis (Fig. 2B). Interestingly, promiscuous activities of UGT51 towards PPD as well as several pharmaceutical sterols and plant sapogenins were observed. UGT51 showed the highest activity towards its natural substrate

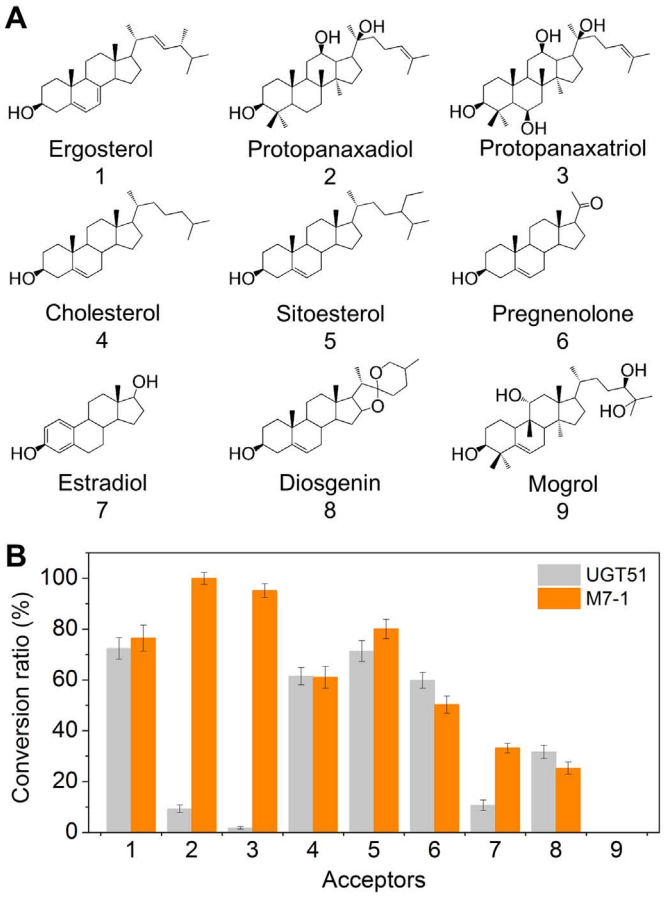

Fig. 2. Acceptor specificity of the recombinant UGT51 and the best mutant M7-1. (A) Chemical structures of the nine acceptors tested. (B) Conversion ratio of each acceptor by the recombinant UGT51 and the best mutant M7-1. The conversion ratios of acceptor substrates were calculated on the basis of remaining acceptors that were quantified by HPLC. The error bars represented the standard deviation from three replicates.

ergosterol and comparable activities towards cholesterol, sitosterol and pregnenolone, which had similar structure with ergosterol. UGT51 could catalyze the glucosylation of PPD and protopanaxatriol (PPT), which contain more hydroxyl group modifications than ergosterol, and they achieved approximately 13% and 2% of the conversion ratio compared with ergosterol, respectively. Mogrol was not catalyzed by UGT51. To confirm the structure of the catalytic product from PPD, the purified product was analyzed via ^{13}C NMR and ^{1}H NMR. The results revealed that UGT51 specifically transferred a glucosyl moiety onto the C-3-OH of PPD and converted it into ginsenoside Rh2 (Fig. S2, S3).

3.2. Semi-rational design of UGT51 toward an efficient Rh2 synthase

Although UGT51 could catalyze the conversion of PPD to Rh2, catalytic activity of the native enzyme was quite low. Semi-rational design guided by structural information serves as an efficient strategy for protein engineering to improve catalytic activity. Thus, we resolved the crystal structure of the catalytic domain of UGT51 with bound UDP-glucose (UDPG) (Chen, et al., unpublished, PDB code: 5gl5). UGT51 displayed the same typical GT-B fold as other reported homologs (Vrielink et al., 1994), and it consisted of two β/α/β Rossmann-like domains that faced each other with the active site lying in the resulting cleft. The UDPG-bound complex revealed that the nucleotide sugar donor bound to the C-terminal domain, whereas the N-terminal domain likely bound the acceptor, PPD. The PPD substrate was docked into the acceptor binding pocket using the automated docking program Autodock 4.2.6 (Morris et al., 2009) (Fig. 3A). The major structural differences of PPD compared with ergosterol (the native substrate for

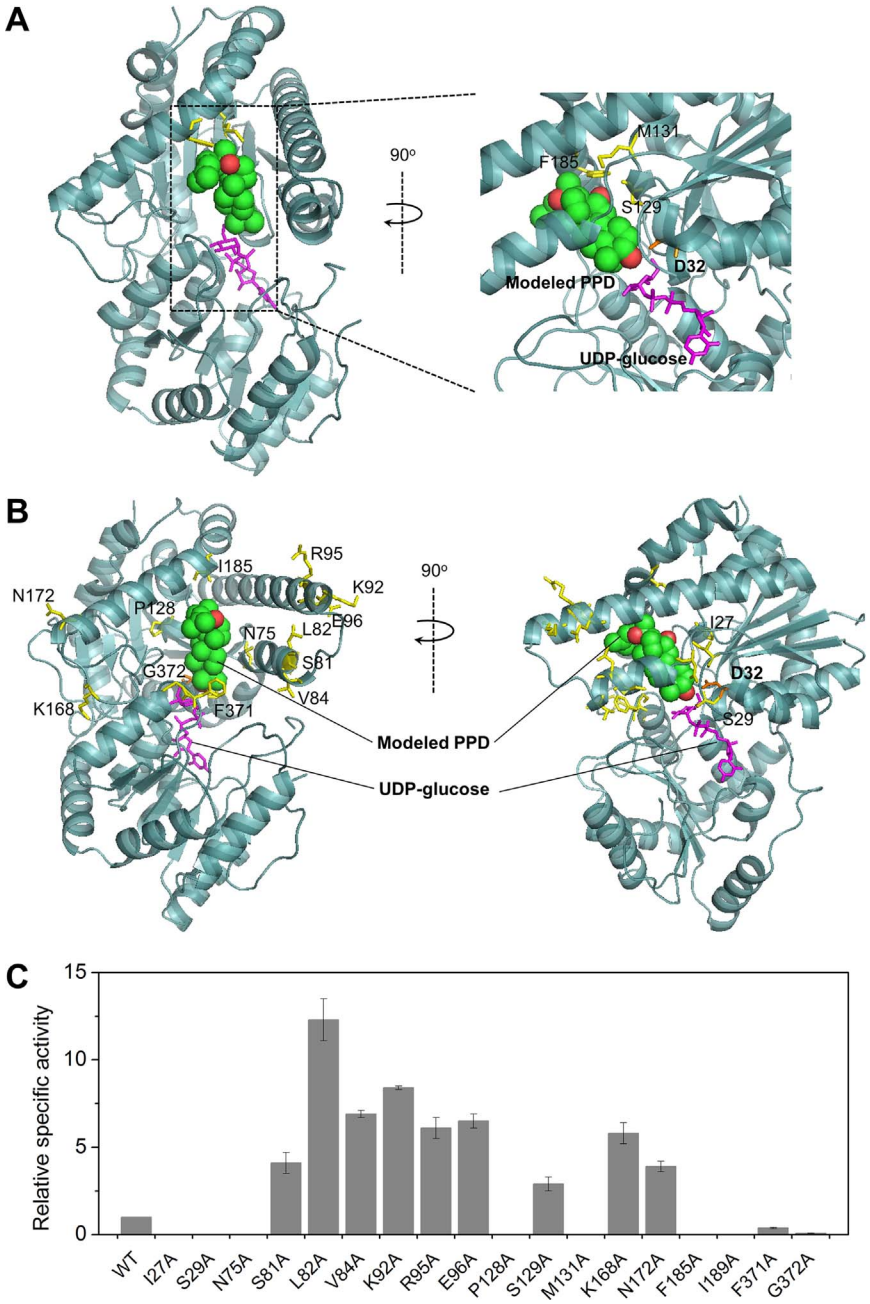

Fig. 3. Potential randomization sites for UGT51 evolution. (A) Overview of the mutagenesis sites designed via a structural analysis at the acceptor binding pocket. (B) Overview of the mutagenesis sites predicted by SEARCHGTr. (C) Relative activities of alanine-substituted mutants of UGT51. The error bars represented the standard deviation from three replicates. (A and B) Randomization sites are shown as yellow sticks. The active residue D32 is shown as an orange stick. The UDP-glucose donor is shown as a magenta stick. The PPD acceptor is shown a green sphere. (For interpretation of the references to color in this figure legend, the reader is referred to the web version of this article.)

UGT51) were the two additional hydroxyl groups at C-12 and C-20. Residues did not directly interact with the hydroxyl group at C-20 because of the outside orientation of this group. Residues S129, M131 and F185, which were located adjacent (3–5 Å) to the C-12 hydroxyl group with hydrophobic interactions, were considered for mutagenesis (Fig. 3A). In addition, because glycosyltransferases undergo significant conformational changes upon substrate binding (Lairson et al., 2008; Qasba et al., 2005), precisely defining the residues related to acceptor binding and catalytic activity is difficult when the crystal structure of the enzyme-acceptor complex is unknown. Therefore, further mutagenesis design was conducted using SEARCHGTr (Kamra et al., 2005) to predict the putative substrate binding residues based on the comprehensive sequence/structure alignment with the reported crystal structures of the glycosyltransferase-acceptor complex. Fifteen residues (I27, S29, N75, S81, L82, V84, K92, R95, E96, P128, K168, N172, I189, F371 and G372) were predicted and selected for mutagenesis (Fig. 3B). We found that most of the residues, including L82, V84, K92, R95, E96, K168 and N172, were located relatively far away (10–20 Å) from the docked PPD molecule, whereas residues I27, S29, and I189 were adjacent (3–5 Å) to PPD, and residues N75, S81, P128, F371 and G372 were 5–10 Å away from PPD.

Alanine scanning was a widespread and rapid technique for examining the contribution of an individual amino acid side chain to the functionality of enzymes (Morrison and Weiss, 2001). The eighteen selected residues were individually mutated to alanine by site-directed mutagenesis and the remaining activities were tested. As shown in Fig. 3C, nine of the 18 mutants (S81A, L82A, V84A, K92A, R95A, E96A, S129A, K168A and N172A) showed higher activity than the wild type.

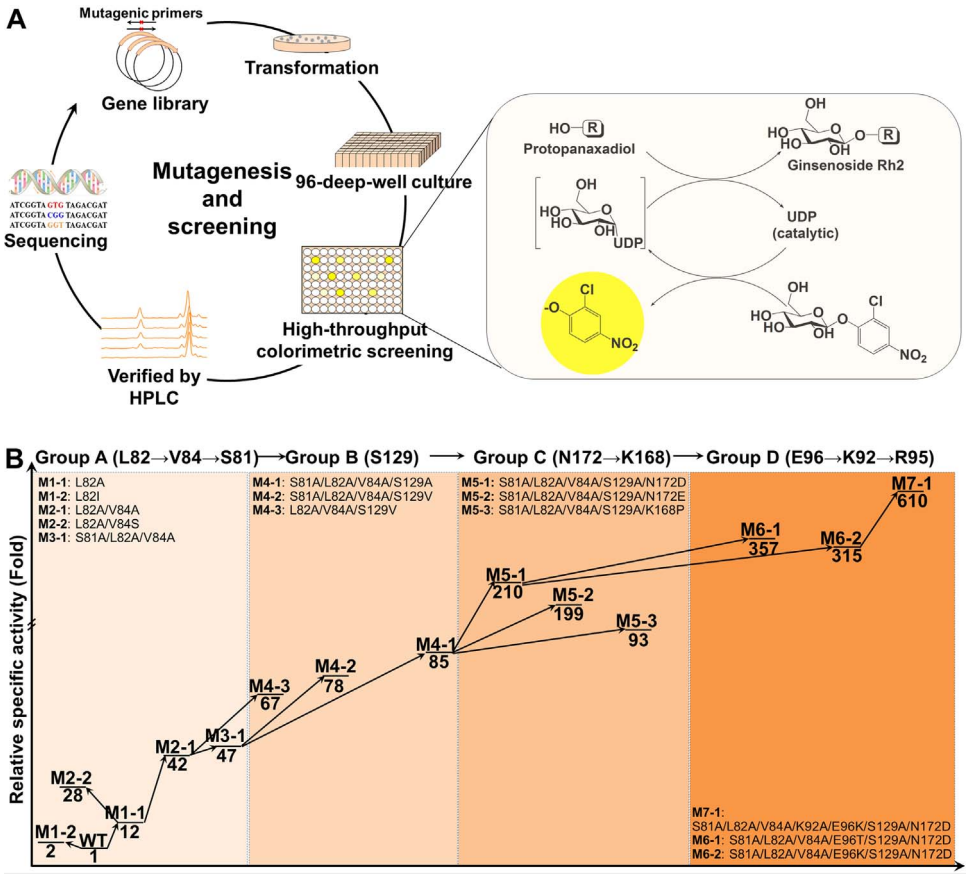

Fig. 4. Evolution of UGT51 towards an efficient Rh2-synthase. (*A*) Schematic of the experimental setup for UGT51 evolution. Dual-glycosyltransferase coupled colorimetric reactions were conducted for high-throughput screening. The glycosyltransferase TDP-16 was used for UDP-glucose generation, resulting in the release of 2-chloro-4-nitrophenolate, which can be followed spectrophotometrically at 410 nm. (*B*) UGT51 evolution was performed by performing nine rounds of iterative saturation mutagenesis along an arbitrarily chosen pathway group A-B-C-D. The numbers below the horizontal lines represent the fold change of the relatively specific activity compared with the wild type.

Table 1
Kinetic parameters of UGT51 and its mutants.

Enzyme	Mutations	K_m (mM)	k_{cat} (s^{-1})	k_{cat}/K_m ($mM^{-1}·s^{-1}$)	Fold change over WT
WT	–	–	–	0.0028 ± 0.0003	1
M3-1	S81A/L82A/V84A	–	–	0.087 ± 0.006	31
M4-1	M3-1 + S129A	–	–	0.12 ± 0.02	43
M5-1	M4-1 + N172D	0.36 ± 0.03	0.49 ± 0.01	1.37 ± 0.03	489
M7-1	M5-1 + E96K/K92A	0.28 ± 0.06	1.40 ± 0.01	5.01 ± 0.09	1789

WT: wild-type
-: Not determined; saturation kinetics could not be attained.

On the other hand, two mutants (F371A and G372A) retained much lower activities (< 40%), while seven mutants (I27A, S29A, N75A, P128A, M131A, F185A and I189A) nearly lost their activities. The mutation sites showing over 60% (Choi et al., 2014) of the relative specific activity compared with the wild-type were chosen for the following saturation mutagenesis. Therefore, the nine positive residues (S81, L82, V84, K92, R95, E96, S129, K168 and N172) were selected. To increase the mutagenesis efficiency, these nine residues were divided into four groups (A, B, C and D) according to their adjacent locations. Iterative saturation mutagenesis (ISM) (Reetz and Carballeira, 2007) was performed on each of the nine residues via an arbitrarily selected pathway (A-B-C-D). A dual-glycosyltransferase colorimetric assay with in situ UDP-glucose regeneration (Gantt et al., 2011) was performed for the high-throughput screening of the glycosyltransferase mutagenesis library (Fig. 4A). The initial hits were verified by HPLC analysis and then sequenced. After nine rounds of iterative mutagenesis as shown in Fig. 4B and screening of ~2800 mutants, the best mutant M7-1 was obtained. M7-1, which contained seven mutations (S81A/L82A/V84A/K92A/E96K/S129A/N172D), achieved 610-fold higher catalytic activity than that of the wild type. The acceptor specificity analysis (Fig. 2B) revealed that mutant M7-1 showed the greatest activity enhancement for PPD and PPT, although the activity was not enhanced toward the natural substrate, ergosterol. The 100% conversion of PPD was achieved by the mutant M7-1 in our *in vitro* condition. Surprisingly, mutant M7-1 displayed a remarkable increase in activity towards PPT, which showed high structural similarity with PPD (53-fold increase of conversion ratio), as well as towards estradiol, which harbored fewer branched group modifications compared with PPD.

The catalytic kinetic performance of the wild type and representative mutants were determined (Table 1). Because of the low solubility of the substrate PPD and the high K_m value, the k_{cat}/K_m values of the wild type and two mutants (M3-1 and M4-1) were estimated under pseudo first-order conditions. Compared with the wild type (0.0028 mM^{-1} s^{-1}),

the catalytic efficiency of mutants M3-1 and M4-1 increased by 31- and 43-fold, respectively. Further mutations of residues in group C and D led to continuous increase of catalytic activities. The k_{cat}/K_m value of the best mutant M7-1 was 1789-fold higher than that of the wild type.

3.3. Production of Rh2 in S. cerevisiae

In order to produce Rh2 directly from glucose or glycerol through microbial fermentation, the native UGT51 and mutant M7-1 genes were individually introduced into *S. cerevisiae* ZD-PPD-016(URA3$^-$) strain (Fig. 1), which was previously engineered for PPD production (Dai et al., 2013). The UGT51 or M7-1 genes under a strong constitutive *TDH3* promoter (P_{TDH3}-*M7-1*-T_{CYC1}) were integrated into the *HO* locus of the ZD-PPD-016(URA3$^-$) strain, resulting in strains ZY-UGT51 and ZY-M7, respectively. Strain ZY-M7 produced 6.08 mg/L Rh2, which was 122-fold higher than that of strain ZY-UGT51.

Although protein engineering of glycosyltransferase led to significant increase of Rh2 production *in vivo*, it was found that large amount of PPD still accumulated. Thus, several metabolic engineering strategies were further used to increase Rh2 production. It was thought Rh2 could be converted back to PPD in yeast by glucosidase, which would decrease Rh2 production. A steryl-beta-glucosidase (EGH1) with broad specificity in *S. cerevisiae* was suggested to be a potential glucosidase. The homolog of EGH1 in *Cryptococcus neoformans*, EGCrP2, had recently been reported to catalyze the reverse reaction of ergosteryl-β-glucoside synthesis, which released ergosterol (Fig. S4A) (Watanabe et al., 2015a, 2015b). Because of the structural similarity between ginsenoside Rh2 and ergosteryl-β-glucoside, we presumed that EGH1 may also hydrolyze ginsenoside Rh2 into PPD. This was demonstrated by *in vitro* enzymatic assay of EGH1. This enzyme showed obvious hydrolytic activity towards Rh2 and achieved a conversion ratio of ~30% at pH 8.0 within 12 h (Fig. S4B). Thus, *EGH1* gene was deleted in strain ZY-M7. The resulting strain ZY-M7(1)-EΔ produced 12.2 mg/L Rh2, which was approximately 2-fold higher than that of strain ZY-M7 (Fig. 5A).

Next, more copies of mutant M7-1 gene were integrated into yeast chromosome to increase glucosyltransferase activity for enhancing Rh2 production. Strain harboring more M7-1 gene copies showed significantly enhanced Rh2 production. However, improvement of Rh2 titer was not linear with the increased copy numbers (Table 2 and Fig. 5A). Strain ZY-M7(4)-EΔ that had four M7-1 gene copies produced 22.2 mg/L Rh2, which was 1.8-fold higher than that of strain ZY-M7(1)-EΔ which had only one M7-1 gene copy.

It was demonstrated that UDP-glucose precursor supply in yeast had a vital role in the biosynthesis of glucoside (Zhou et al., 2011). RT-PCR analysis of *HXK1, PGM1* and *UGP1* genes which were involved in UDP-glucose biosynthesis were performed. As shown in Fig. 5C, the last two genes, especially *PGM1*, exhibited extremely low transcriptome levels, implying that these might be rate-limiting steps for UDP-glucose precursor supply and Rh2 production. Thus, both *PGM1* and *UGP1* genes were overexpressed by introducing additional gene copies under the *PGK1* and *HXT7* promoter, respectively. The resulting strain ZY-M7(4)-EΔ-PU produced 36.7 mg/L Rh2, which was 65% higher than that of the parent strain ZY-M7(4)-EΔ (Table 2).

In addition, all yeast strains constructed in our study accumulated high amounts of dammarenediol II (more than 7 mg/g DCW). The conversion of dammarenediol II to PPD was catalyzed by P450 (*PgPPDS*) and its reductase, ATR1, in our engineered strains. Previous studies demonstrated that the cytochrome P450 reductase ATR2 was more efficient than ATR1 (Schuckel et al., 2012; Wang et al., 2015). In addition, because of the high efficiency of self-sufficient P450 (Zhao et al., 2016), gene cassette *PPDS-75tATR2*, which encoded self-sufficient P450 fusion proteins, was integrated into the *δ* site of strain ZY-M7(4)-EΔ-PU(URA3$^-$). The resulting strain ZY-M7(4)-EΔ-PUA produced 45 mg/L Rh2, which was 20% higher than that of the parent strain ZY-M7(4)-EΔ-PU (Table 2 and Fig. 5B). The structures of Rh2 and its precursors produced by ZY-M7(4)-EΔ-PUA were further confirmed by HPLC/ESIMS (Fig. S5).

To assess the industrial performance of the final strain ZY-M7(4)-EΔ-PUA, a fed-batch fermentation was conducted in a 5-L bioreactor. The fermentation batch phase began with 25 g/L glucose. Feeding was initiated after glucose was depleted (~36 h after inoculation). Cell growth reached the exponential stage after 48 h and continued to increase until 120 h. A maximum OD_{600} of 384 was obtained. Rh2 production increased with continued cell growth and the maximum titer (292 mg/L) was obtained at 120 h (Fig. 5D). To our knowledge, this was the highest titer reported to date.

4. Discussion

Advances in synthetic biology have enabled tailored production of plant natural products in microorganisms. However, many natural products derived from plant secondary metabolism cannot be synthesized in the microbial chassis because of shortages of valid and identified synthetic genes, which are difficult to be characterized because of their dispersed distributions in the plant chromosome. On the other hand, many plant derived enzymes are difficult to be optimally expressed in microbial hosts (Chen and Halkier, 1999; Galanie et al., 2015), leading to low product yields. The replacement of native plant enzymes with engineered promiscuous microbial enzymes represents an alternative and promising strategy to overcome these issues. In this study, the promiscuous UGT51 from *S. cerevisiae* was successfully repurposed into an efficient glycosyltransferase for ginsenoside Rh2 synthesis via semi-rational design, and it achieved an ~1800-fold improved k_{cat}/K_m value. Our findings provide insights into the development of a new enzyme reservoir by using the unique but popular characteristics of microbial enzyme promiscuity.

Although UGT51 showed a distant evolutionary relationship with the ginseng sapogenin glycosyltransferase UGTPg45 (sequence homology = 24.8%, Fig. S6), the best mutant M7-1, which has seven mutations, possesses a similar K_m value (280 μM) and a 3.6-fold higher k_{cat} value (1.40 s^{-1}) compared with UGTPg45 (209 μM and 0.38 s^{-1}) (Wang et al., 2015). The best mutant M7-1 was achieved after screening less than 3000 mutants, which was facilitated by semi-rational design. An analysis of the structure of UGT51 suggested that six of the seven beneficial mutation sites (S81, L82, V84, K92, E96 and N172) in M7-1 were located 9–20 Å away from the docked substrate, implying that these residues may be involved in a significant conformational change upon substrate binding.

UGT51 exhibits remarkably broad substrate specificity towards a range of important sapogenins (Fig. 2). To our knowledge, UGT51 represents one of the most promiscuous sterol glucosyltransferases to date and is the first glucosyltransferase that catalyzes the glucosylation of pregnenolone. During the semi-rational design process, the substrate specificity of UGT51 appeared to become more promiscuous. When the best mutant M7-1 showed substantially enhanced catalytic activity towards the screening substrate PPD, its activity for PPT and estradiol were also obviously improved. Further molecular design may lead to the development of an enzyme with even broader substrate specificity that could serve as a general glycosylation platform for various valuable sapogenins, and this approach would be useful for the biosynthesis of other plant saponins, especially those whose native glycosyltransferase genes have not yet been identified.

Introducing the mutant glycosyltransferase M7-1 gene into *S. cerevisiae* led to 122-fold increase of Rh2 production (from 0.0032 to 0.39 mg/g DCW). However, this improvement was not comparable to the increased glycosyltransferase activity *in vitro* (~1800-fold). Two limiting factors for efficient Rh2 production in *S. cerevisiae* were identified. The first one was Rh2 degradation. Rh2 was hydrolyzed back to PPD by a reverse reaction *in vivo*. After a comparative analysis of the pathway for ergosteryl-glucoside degradation by β-glucosidase in yeast, we identified a latent glycosidase EGH1. After blocking Rh2

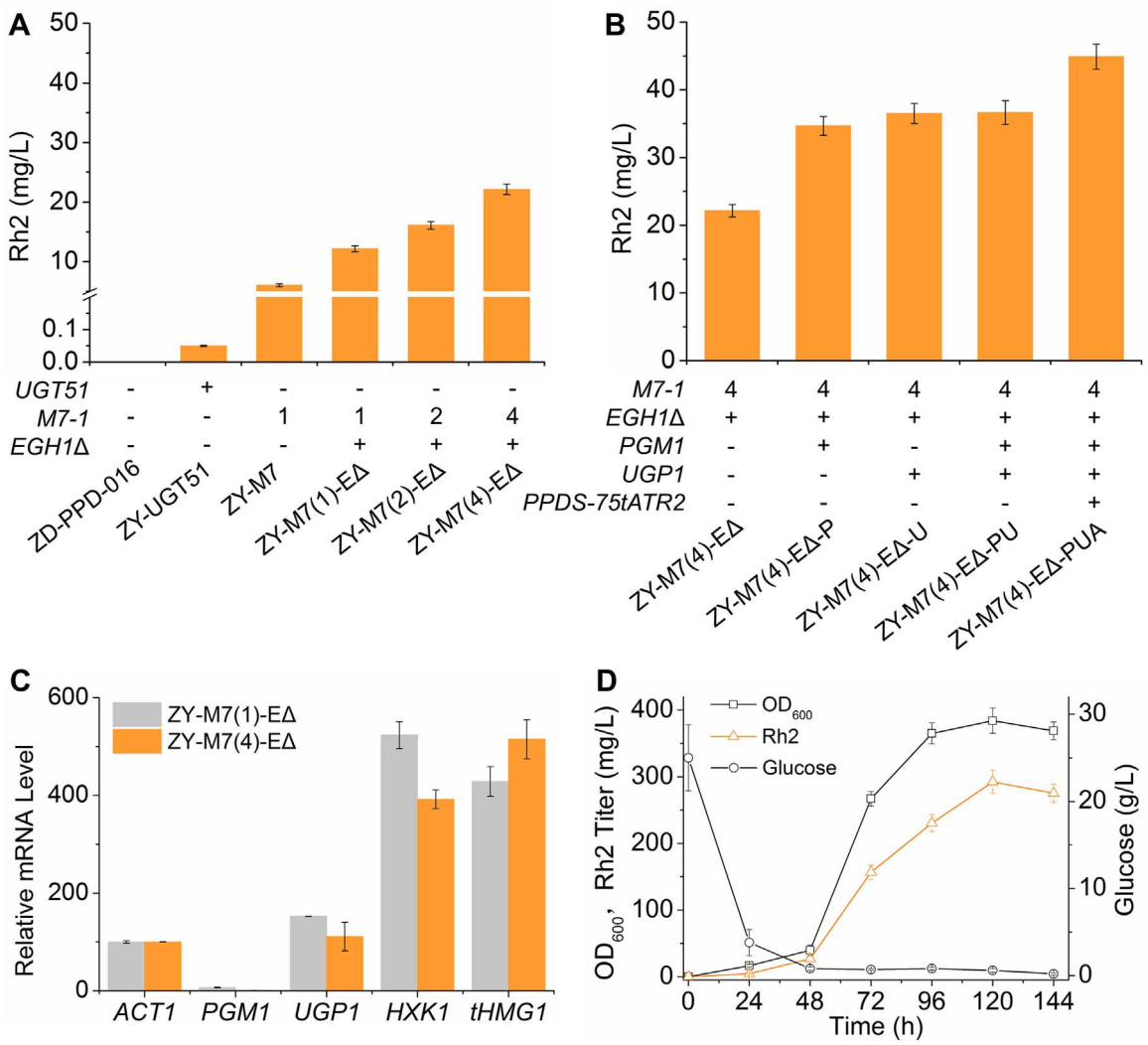

Fig. 5. Production of ginsenoside Rh2 via engineered *S. cerevisiae* strains. (*A*) (*B*) Rh2 titers obtained from the engineered strains cultured in shake flasks. *PPDS-75tATR2*: The PPDS domain was linked with a truncated ATR2 reductase domain. *PGM1*: phosphoglucomutase gene; and *UGP1*: UDP-glucose pyrophosphorylase gene. (*C*) Transcriptional profiling of the genes involved in UDP-glucose biosynthesis in the engineered strains. The mRNA level of the internal reference gene *ACT1* was considered 100%. *ACT1*: actin gene; *HXK1*: hexokinase gene; and *tHMG1*: truncated HMG-CoA reductase gene, which was overexpressed in the chassis cell. (*D*) Production of ginsenoside Rh2 by strain ZY-M7(4)EΔ-PUA via fed-batch fermentation. (*A-D*) Error bars represented the standard deviation from three replicates.

Table 2
Production of ginsenoside Rh2 and precursor products by the engineered strains.

Strains[a]	DCW (g/L)	DDII (mg/g DCW)	PPD (mg/g DCW)	Rh2 (mg/g DCW)
ZD-PPD-016(URA3$^-$)	15.66 ± 0.79	10.36 ± 0.32	8.01 ± 0.89	0
ZY-UGT51	15.53 ± 0.77	10.40 ± 0.52	7.99 ± 0.77	0.0032 ± 0.0005
ZY-M7	15.58 ± 0.90	9.89 ± 0.45	7.69 ± 0.66	0.39 ± 0.09
ZY-M7(1)-EΔ	15.03 ± 0.88	9.71 ± 0.38	7.43 ± 0.59	0.81 ± 0.05
ZY-M7(2)-EΔ	15.18 ± 0.75	8.42 ± 0.45	6.48 ± 0.36	1.06 ± 0.11
ZY-M7(4)-EΔ	15.39 ± 0.82	7.12 ± 0.55	4.86 ± 0.42	1.44 ± 0.10
ZY-M7(4)-EΔ-PU	15.60 ± 0.88	7.25 ± 0.68	4.96 ± 0.85	2.35 ± 0.17
ZY-M7(4)-EΔ-PUA	15.49 ± 0.96	6.50 ± 0.62	5.33 ± 0.59	2.90 ± 0.18

DCW: dry cell weight; DDII: dammarenediol II; and PPD: protopanaxadiol.
[a] Three replicates were performed for each strain, and the error bars represented the standard deviation from three replicates.

degradation by deleting *EGH1* gene, Rh2 titer increased by approximately 2 times. Sufficient supply of UDP-glucose precursor was another limiting factor for efficient Rh2 production *in vivo*. Overexpression of *PGM1* and *UGP1* genes to improve UDP-glucose supply led to additional 63% increase of Rh2 production in engineered *S. cerevisiae*.

In conclusion, we have successfully achieved the highest titer (~300 mg/L) of Rh2 production in *S. cerevisiae* to date via combining protein engineering of an inherently promiscuous glycosyltransferase and metabolic engineering. The wide substrate spectra of the glycosyltransferase mutant and the robustness of the yeast chassis provided a new route for synthesizing other important plant saponins.

Acknowledgements

This work was supported by the Science and Technology Commission of Shanghai Municipality (15JC1400402) and the National Basic Research Program of China (973 Program, grant no. 2012CB721000). Science and Technology Commission of Shanghai Municipality. We thank Prof. Hongwei Yu (Zhejiang University) for kindly sharing the plasmid pUMRI-10. We thank Dr. Lishan Zhao, Prof. Shuangjun Lin and Prof. Wen Liu for helpful comments for manuscript writing.

Appendix A. Supporting information

Supplementary data associated with this article can be found in the online version at http://dx.doi.org/10.1016/j.ymben.2017.04.009.

References

Ajikumar, P.K., Xiao, W.H., Tyo, K.E.J., Wang, Y., Simeon, F., Leonard, E., Mucha, O., Phon, T.H., Pfeifer, B., Stephanopoulos, G., 2010. Isoprenoid Pathway optimization for taxol precursor overproduction in *Escherichia coli*. Science 330, 70–74.

Bae, E.A., Han, M.J., Kim, E.J., Kim, D.H., 2004. Transformation of ginseng saponins to ginsenoside Rh2 by acids and human intestinal bacteria and biological activities of their transformants. Arch. Pharm. Res. 27, 61–67.

Brown, S., Clastre, M., Courdavault, V., O'Connor, S.E., 2015. De novo production of the plant-derived alkaloid strictosidine in yeast. Proc. Natl. Acad. Sci. USA 112, 3205–3210.

Chen, S., Halkier, B.A., 1999. Functional expression and characterization of the Myrosinase MYR1 from *Brassica napus* in *Saccharomyces cerevisiae*. Protein Expres Purif. 17, 414–420.

Choi, Y.H., Kim, J.H., Park, J.H., Lee, N., Kim, D.H., Jang, K.S., Park, I.H., Kim, B.G., 2014. Protein engineering of alpha2,3/2,6-sialyltransferase to improve the yield and productivity of *in vitro* sialyllactose synthesis. Glycobiology 24, 159–169.

Copley, S.D., 2015. An evolutionary biochemist's perspective on promiscuity. Trends Biochem. Sci. 40, 72–78.

Dai, Z.B., Liu, Y., Zhang, X.A., Shi, M.Y., Wang, B.B., Wang, D., Huang, L.Q., Zhang, X.L., 2013. Metabolic engineering of *Saccharomyces cerevisiae* for production of ginsenosides. Metab. Eng. 20, 146–156.

Dietrich, J.A., Yoshikuni, Y., Fisher, K.J., Woolard, F.X., Ockey, D., McPhee, D.J., Renninger, N.S., Chang, M.C.Y., Baker, D., Keasling, J.D., 2009. A novel semi-biosynthetic route for Artemisinin production using engineered substrate-promiscuous $P450_{BM3}$. ACS Chem. Biol. 4, 261–267.

Galanie, S., Thodey, K., Trenchard, I.J., Interrante, M.F., Smolke, C.D., 2015. Complete biosynthesis of opioids in yeast. Science 349, 1095–1100.

Gantt, R.W., Peltier-Pain, P., Cournoyer, W.J., Thorson, J.S., 2011. Using simple donors to drive the equilibria of glycosyltransferase-catalyzed reactions. Nat. Chem. Biol. 7, 685–691.

Hwang, J.T., Kim, S.H., Lee, M.S., Kim, S.H., Yang, H.J., Kim, M.J., Kim, H.S., Ha, J., Kim, M.S., Kwon, D.Y., 2007. Anti-obesity effects of ginsenoside Rh2 are associated with the activation of AMPK signaling pathway in 3T3-L1 adipocyte. Biochem. Biophys. Res. Commun. 364, 1002–1008.

Kamra, P., Gokhale, R.S., Mohanty, D., 2005. SEARCHGTr: a program for analysis of glycosyltransferases involved in glycosylation of secondary metabolites. Nucleic Acids Res. 33, W220–225.

Kim, H.E., Oh, J.H., Lee, S.K., Oh, Y.J., 1999. Ginsenoside RH-2 induces apoptotic cell death in rat C6 glioma via a reactive oxygen- and caspase-dependent but Bcl-X_L-independent pathway. Life Sci. 65, 33–40.

Kitagawa, I., Yoshikawa, M., Yoshihara, M., Hayashi, T., Taniyama, T., 1983. Chemical studies of crude drugs (1). Constituents of Ginseng radix rubra. Yakugaku zasshi. 103, 612–622.

Lairson, L.L., Henrissat, B., Davies, G.J., Withers, S.G., 2008. Glycosyltransferases: structures, functions, and mechanisms. Annu. Rev. Biochem. 77, 521–555.

Lenihan, J.R., Tsuruta, H., Diola, D., Renninger, N.S., Regentin, R., 2008. Developing an Industrial Artemisinic Acid Fermentation Process to Support the Cost-Effective Production of Antimalarial Artemisinin-Based Combination Therapies. Biotechnol. Prog. 24, 1026–1032.

Liu, Z.Q., 2012. Chemical insights into ginseng as a resource for natural antioxidants. Chem. Rev. 112, 3329–3355.

Martin, V.J., Pitera, D.J., Withers, S.T., Newman, J.D., Keasling, J.D., 2003. Engineering a mevalonate pathway in *Escherichia coli* for production of terpenoids. Nat. Biotechnol. 21, 796–802.

Morris, G.M., Huey, R., Lindstrom, W., Sanner, M.F., Belew, R.K., Goodsell, D.S., Olson, A.J., 2009. AutoDock4 and AutoDockTools4: automated docking with selective receptor flexibility. J. Comput. Chem. 30, 2785–2791.

Morrison, K.L., Weiss, G.A., 2001. Combinatorial alanine mutagenesis. Curr. Opin. Chem. Biol. 5, 302–307.

Nakata, H., Kikuchi, Y., Tode, T., Hirata, J., Kita, T., Ishii, K., Kudoh, K., Nagata, I., Shinomiya, N., 1998. Inhibitory effects of ginsenoside Rh-2 on tumor growth in nude mice bearing human ovarian cancer cells. Jpn. J. Cancer Res. 89, 733–740.

Qasba, P.K., Ramakrishnan, B., Boeggeman, E., 2005. Substrate-induced conformational changes in glycosyltransferases. Trends Biochem. Sci. 30, 53–62.

Reetz, M.T., Carballeira, J.D., 2007. Iterative saturation mutagenesis (ISM) for rapid directed evolution of functional enzymes. Nat. Protoc. 2, 891–903.

Schuckel, J., Rylott, E.L., Grogan, G., Bruce, N.C., 2012. A gene-fusion approach to enabling plant cytochromes p450 for biocatalysis. Chembiochem 13, 2758–2763.

Shibata, S., 2001. Chemistry and cancer preventing activities of ginseng saponins and some related triterpenoid compounds. J. Korean Med. Sci. 16, Suppl, S28–37.

Su, J.H., Xu, J.H., Lu, W.Y., Lin, G.Q., 2006. Enzymatic transformation of ginsenoside Rg3 to Rh2 using newly isolated *Fusarium proliferatum* ECU2042. J. Mol. Catal. B-Enzym. 38, 113–118.

Vrielink, A., Ruger, W., Driessen, H.P., Freemont, P.S., 1994. Crystal structure of the DNA modifying enzyme beta-glucosyltransferase in the presence and absence of the substrate uridine diphosphoglucose. Embo J. 13, 3413–3422.

Wang, P., Wei, Y., Fan, Y., Liu, Q., Wei, W., Yang, C., Zhang, L., Zhao, G., Yue, J., Yan, X., Zhou, Z., 2015. Production of bioactive ginsenosides Rh2 and Rg3 by metabolically engineered yeasts. Metab. Eng. 29, 97–105.

Warnecke, D., Erdmannn, R., Fahl, A., Hube, B., Muller, F., Zank, T., Zahringer, U., Heinz, E., 1999. Cloning and functional expression of UGT genes encoding sterol glucosyltransferases from *Saccharomyces cerevisiae*, *Candida albicans*, *Pichia pastoris*, and *Dictyostelium discoideum*. J. Biol. Chem. 274, 13048–13059.

Watanabe, T., Ishibashi, Y., Ito, M., 2015a. Physiological significance of glycolipid catabolism in *Cryptococcus neoformans*. Trends Glycosci. Glyctechnol. 27, E21–31.

Watanabe, T., Ito, T., Goda, H.M., Ishibashi, Y., Miyamoto, T., Ikeda, K., Taguchi, R., Okino, N., Ito, M., 2015b. Sterylglucoside catabolism in *Cryptococcus neoformans* with endoglycoceramidase-related protein 2 (EGCrP2), the first steryl-beta-glucosidase identified in fungi. J. Biol. Chem. 290, 1005–1019.

Xie, W., Lv, X., Ye, L., Zhou, P., Yu, H., 2015. Construction of lycopene-overproducing Saccharomyces cerevisiae by combining directed evolution and metabolic engineering. Metab. Eng. 30, 69–78.

Zhang, C.Z., Yu, H.S., Bao, Y.M., An, L.J., Jin, F.X., 2001. Purification and characterizationof ginsenoside-beta-glucosidase from ginseng. Chem. Pharm. Bull. 49, 795–798.

Zhao, F., Bai, P., Liu, T., Li, D., Zhang, X., Lu, W., Yuan, Y., 2016. Optimization of a cytochrome P450 oxidation system for enhancing protopanaxadiol production in *Saccharomyces cerevisiae*. Biotechnol. Bioeng. 113, 1787–1795.

Zhou, X., Wu, H., Li, Z., Zhou, X., Bai, L., Deng, Z., 2011. Over-expression of UDP-glucose pyrophosphorylase increases validamycin A but decreases validoxylamine A production in *Streptomyces hygroscopicus* var. *jinggangensis* 5008. Metab. Eng. 13, 768–776.